ELSEVIER

Journal of Alloys and Compounds 275–277 (1998) 578–582

Journal of ALLOYS AND COMPOUNDS

Magnetic structure of $TbIrSi_3$ compound

W. Bażela[a], N. Stüsser[b], A. Szytuła[c,*], A. Zygmunt[d]

[a]*Institute of Physics, Cracow University of Technology, Kraków, Poland*
[b]*BENSC Hahn-Meitner Institute, Berlin-Wannsee, Germany*
[c]*Institute of Physics, Jagellonian University, Reymonta 4, 30-059 Kraków, Poland*
[d]*W. Trzebiatowski Institute of Low Temperatures and Structural Research, Polish Academy of Sciences, Wrocław, Poland*

Abstract

The paper reports on neutron diffraction and magnetic measurements of $TbIrSi_3$. The compound crystallizes in the tetragonal $BaNiSn_3$-type of structure. Below 16 K, the Tb-magnetic moments order antiferromagnetically. In the temperature region 1.6–7.4 K, a collinear antiferromagnetic structure of AFI-type with the moment in the basal plane is observed. With increasing temperature, the magnetic structure changes into a transversal sine-wave modulated structure. In the temperature region 7.8–11 K, a collinear and a sine-modulated structure coexist whereas in the region 11–16 K, a sine-modulated one is detected. The data are briefly discussed in terms of the RKKY theory and electric-field model. © 1998 Elsevier Science S.A.

Keywords: Rare earth intermetallic; Neutron powder diffraction; Magnetic structure; Phase transition

1. Introduction

From the $BaAl_4$ structure [1], three types of crystal structure have been derived: $ThCr_2Si_2$ [2] or $CeAl_2Ge_2$ [3], $CaBe_2Ge_2$ [4] and $BaNiSn_3$ [5]. The magnetic properties of RT_2X_2 (R=rare earth, T=transition metal, X=Si,Ge,Sn,Sb) have been investigated intensively in recent years [6,7]. Little is known about the magnetic properties of the RTX_3 compounds. It was shown that $LaRhSi_3$, $LaIrSi_3$ and $CeCoSi_3$ are superconducting whereas $CeRhSi_3$ and $CeIrSi_3$ have Kondo-lattice characteristics [8]. $GdIrSi_3$ and $DyIrSi_3$ are antiferromagnets with the Néel temperatures of 11.5 and 7.5 K, respectively. ^{155}Gd Mössbauer data show that the Gd moments are aligned in the basal plane. The ^{161}Dy Mössbauer data imply the occurrence of an incommensurate spin structure in $DyIrSi_3$ [9]. Below 11 K, $TbRhSi_3$ orders antiferromagnetically with the noncollinear magnetic structure [10].

The present study reports on magnetic and neutron diffraction measurements on polycrystalline samples of $TbIrSi_3$.

2. Experimental procedure

The $TbIrSi_3$ sample was prepared using stoichiometric amounts of the constituent elements by arc melting under a purified argon atmosphere and by the subsequent vacuum annealing at 950°C for one week.

The sample was analyzed by the X-ray diffraction using the CuKα radiation. The lattice parameters $a=4.141(5)$ Å and $c=9.659(3)$ Å are in good agreement with those reported previously [11].

The magnetization data were collected by means a vibrating sample-magnetometer in magnetic fields up to 50 kOe. A SQUID magnetometer was adopted to perform additional measurements in low magnetic fields.

The neutron diffraction experiments were carried out with the E6 diffractometer installed at the BERII reactor at the Hahn–Meitner Institute, Berlin. Several patterns were recorded in the temperature range 1.6–20 K. The incident neutron wavelength was 2.422 Å. The data were processed by the Rietveld method using the FULLPROF program [12] with scattering lengths taken from reference [13] and the Tb^{3+} form factor was adopted from reference [14].

The magnetization vs. temperature curve obtained in the presence of external magnetic fields 50 and 100 Oe indicates the Néel temperature at 16 K and an additional magnetic phase transition at $T_t=10$ K (Fig. 1a). The measurement in a magnetic field of 10 kOe gives a small reduction of the Néel temperature value (Fig. 1b). Above the Néel temperature, the reciprocal magnetic susceptibility vs temperature obeys the Curie-Weiss law (see Fig. 1c) with a negative value of the paramagnetic Curie

*Corresponding author. E-mail: szytula@if.uj.edu.pl

0925-8388/98/$19.00 © 1998 Elsevier Science S.A. All rights reserved.
PII: S0925-8388(98)00395-8

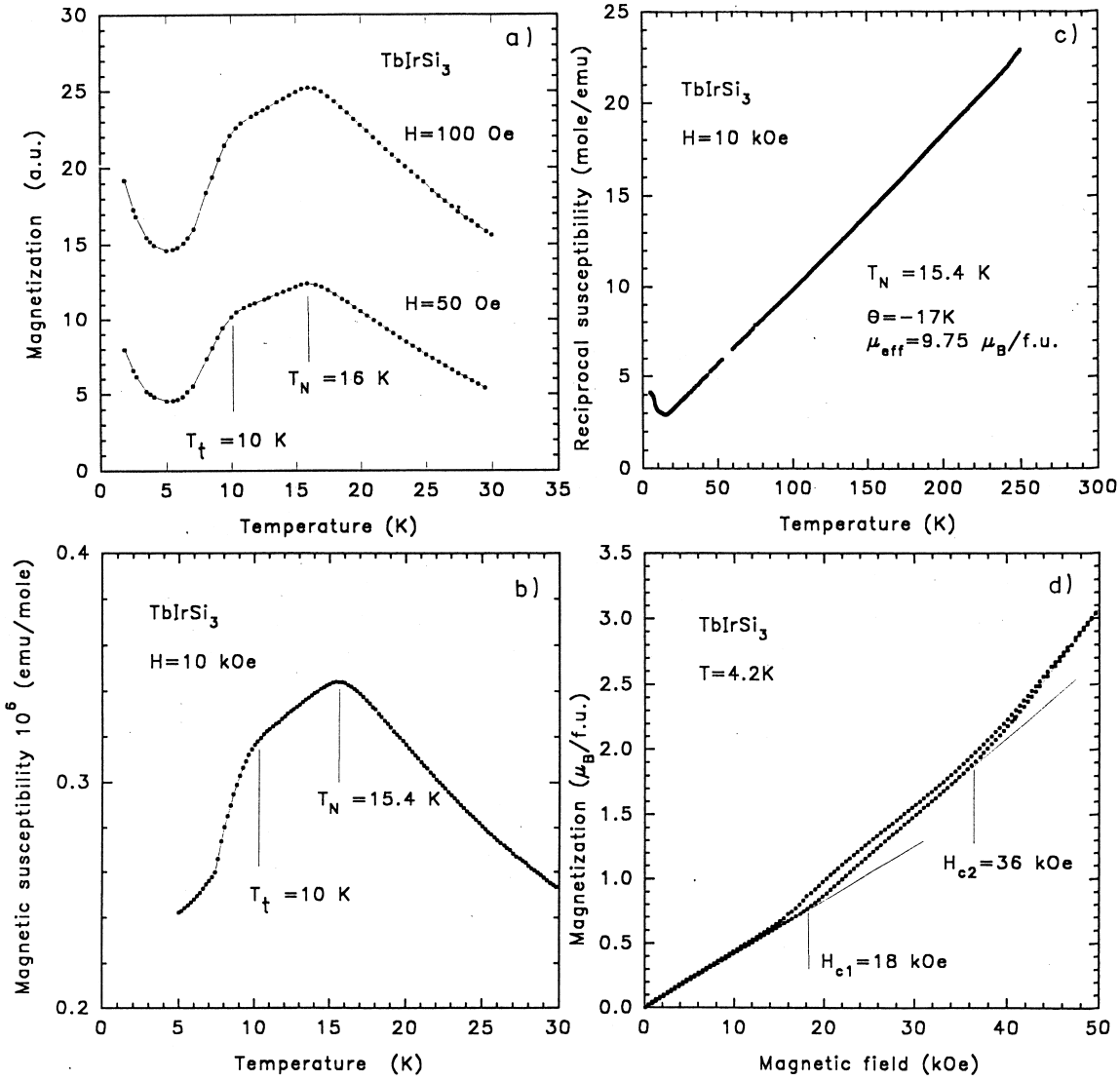

Fig. 1. The temperature dependencies of the (a) magnetization at low-magnetic field, (b) magnetic susceptibility and (c) reciprocal magnetic susceptibility in magnetic field $H=10$ kOe and magnetization vs. magnetic field strength function recorded at 4.2 K for $TbIrSi_3$.

temperature $\theta_p=-17$ K and the paramagnetic moment on Tb^{3+} ion amounting to 9.75 μ_B i.e. very close to its free-ion value of 9.72 μ_B. The magnetization curves at 4.2 K as a function of the applied magnetic field show a metamagnetic character with the critical field $H_{C1}=18$ kOe and $H_{C2}=36$ kOe (Fig. 1d).

The neutron diffractogram recorded at $T=20$ K (see Fig. 2) contains reflections with $h+k+l$ even, confirming the space group *I4mm*, with the Tb, Ir, and Si_1 atoms located at the 2(a) site: $(0,0,z_i)$ and Si_2 at the 4(b) site: $(0,1/2,z_4)$; $(1/2,0,z_4)$;+body centering translation. The z_i-free parameters were determined and refined using the nuclear reflections. They are listed in Table 1.

The observed magnetic peaks at $T=1.6$ K have $h+k+l=2n+1$. This suggests a collinear antiferromagnetic structure of the AFI-type [7]. The magnetic unit cell is of the same dimension as the crystallographic one. The existence of the 001 magnetic peak indicates that the magnetic moment has a component perpendicular to the *c*-axis. The refinement has shown that the Tb-magnetic moments form ferromagnetic planes perpendicular to the *c*-axis. The coupling between adjacent planes however is antiferromagnetic (see Fig. 3a). Such a magnetic ordering is observed up to $T=7.4$ K.

At $T=7.8$ K, additional peaks appear and they can be indexed as satellites of the magnetic peaks with a propagation vector $k=(0,0,k_z)$. With increasing temperature, the intensities of the main magnetic peaks decrease while those of the satellites increase. The numerical analysis of the magnetic peaks gives a sine-modulated magnetic structure (see Fig. 3b).

The analysis of all neutron diffraction patterns taken in the temperature region between 1.6 and 20 K gives the following magnetic structures:

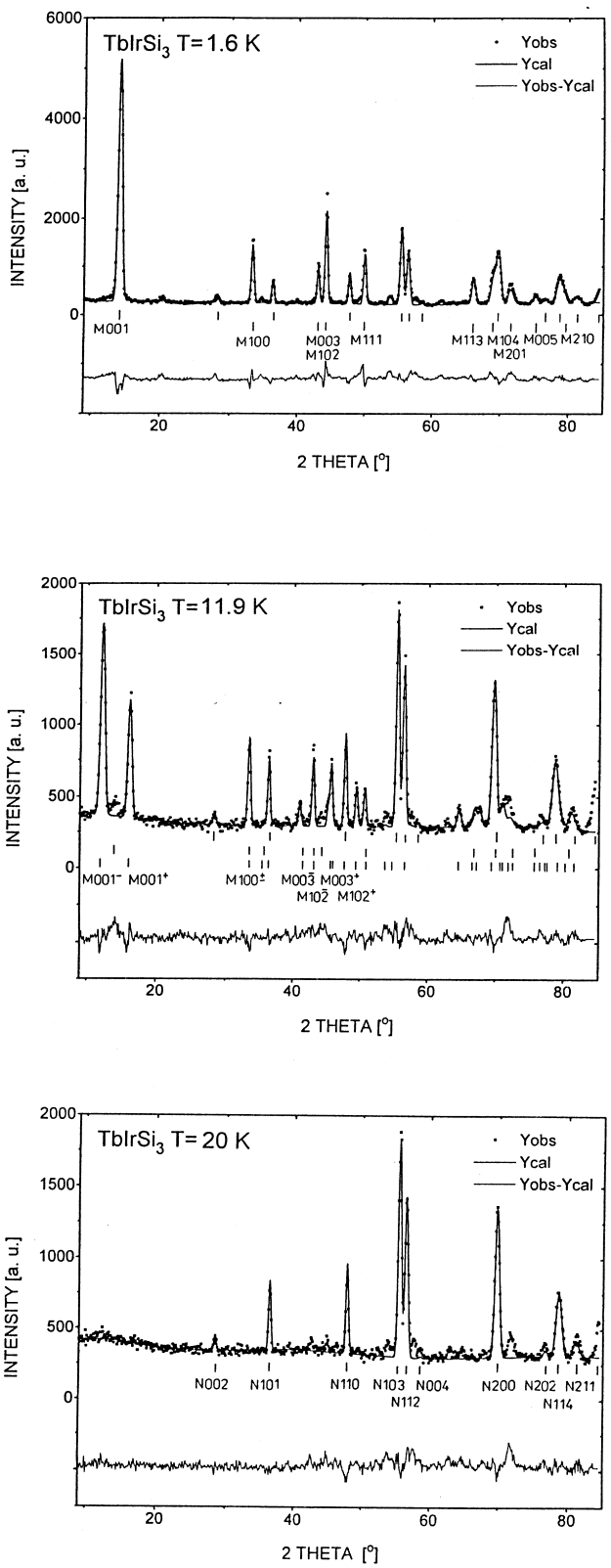

Fig. 2. The observed neutron diffraction patterns of $TbIrSi_3$ obtained at 1.6, 11.9 and 20 K and the calculated profiles represented by the solid lines. Difference patterns are shown below. The ticks indicate the positions of the nuclear (upper row) and the magnetic reflections corresponding to the collinear and sine-modulated structures (lower rows) used in the profile analysis.

Table 1
Crystal data for $TbIrSi_3$ at $T=20$ K

a(Å)	4.2453(6)
c(Å)	9.9316(20)
a/c	0.4274
z_{Tb}	0 (fixed)
z_{Ir}	0.641(5)
z_{Si1}	0.393(7)
z_{Si2}	0.771(7)
R_{Bragg} (%)	7.8
R_{prof} (%)	6.8

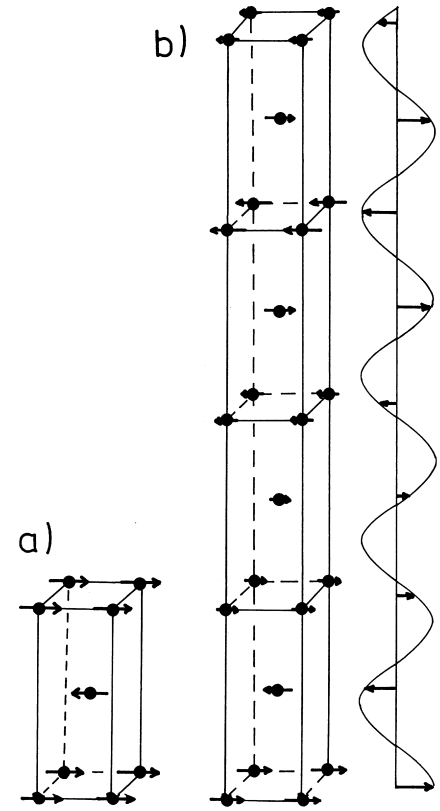

Fig. 3. A schematic representation of the magnetic structures of $TbIrSi_3$ at different temperatures: (a) a collinear AFI-type (1.6 K$\leq T\leq$7.4 K), and (b) sine modulated (11 K$<T<T_N=$16 K). Only the Tb atoms are presented.

- in the region 1.6–7.4 K, a collinear antiferromagnetic ordering,
- in the region 7.8–11 K, a coexistence of a collinear and a sine-wave-modulated magnetic structure,
- in the region 11 K up to 16 K, a sine-wave-modulated magnetic ordering (see Fig. 3b).

The temperature dependencies of the total magnetic moment as well as of the collinear and the sine-modulated components are presented in Fig. 4a.

An anomalous dependence of the z-component of the propagation vector is observed in the region 7.8–16 K. At $T=7.8$ K, the z-component is equal to 6/7. With an increase of the temperature, the k_z value first increases up

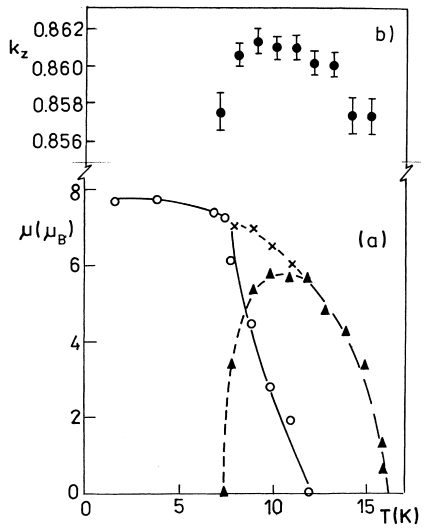

Fig. 4. Temperature dependence of the: (a) total magnetic moment (×) and collinear (○) and helicoidal (▲) components and (b) propagation vector k_z component of the magnetic moment.

to 0.861 and then decreases up to 6/7 (0.857) (see Fig. 4b).

Fig. 5 shows the temperature variations of the lattice parameters *a* and *c*, of the *c*/*a* ratio and of the unit cell volume *V*. In the temperature near 8 K, the *a*-constant and the volume *V* decrease while the *c*/*a* ratio increases.

3. Discussion

The $TbIrSi_3$ compound crystallizes in the $BaNiSn_3$-type of tetragonal structure which is closely related to the $ThCr_2Si_2$ (*I*-form, space group *I4*/*mmm*) or in the $CaBe_2Ge_2$ (*P*-form, space group *P4*/*nmm*) type of structures. They differ only in the stacking of alternate layers:

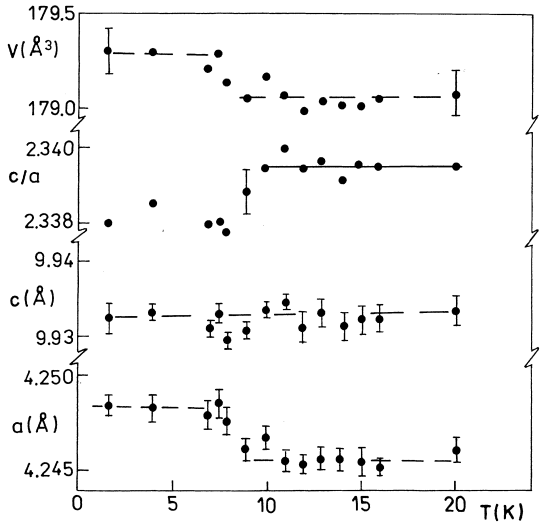

Fig. 5. The temperature dependence of the lattice parameters *a* and *c*, the *a*/*c* ratio, and the unit cell volume *V* for $TbIrSi_3$.

Tb-Si-Ir-Si-Tb-Si-Ir-Si for $ThCr_2Si_2$-type
Tb-Ir-Si-Ir-Tb-Si-Ir-Si for $CaBe_2Ge_2$-type, and
Tb-Ir-Si-Si-Tb-Ir-Si-Si for $BaNiSn_3$-type (see Fig. 6).

Both forms of $TbIr_2Si_2$ are antiferromagnetic, the *I*-form with T_N=80 K and θ_p=+42 K and the *P*-form with T_N=13 K and θ_p=+13 K [15].

Only the *I*-form was studied by the neutron diffraction [16]. A collinear, antiferromagnetic ordering of AFI-type with the magnetic moments aligned along the tetragonal axis [propagation vector k=(0,0,1)] was found.

Since the Tb-Tb interplane (~4.25 Å) and intraplane (~5.8 Å) distances in $TbIrSi_3$ are large, the stability of the observed magnetic structures are realized by the indirect interactions via conduction electrons (the RKKY model). These distances are similar in both phases, a change in the density of states at Fermi level (RKKY-type interaction) can explain small T_N and θ_p values observed in the P-form. The distribution of the atoms and the Néel temperature of $TbIrSi_3$ are similar to those observed in P-form of $TbIr_2Si_2$.

The observed magnetic ordering of the Tb-moments in $TbIrSi_3$ is similar to that observed in the *I*-form of $TbIr_2Si_2$ (AFI-type). The orientation of the magnetic moments, however, differ: in *I*-$TbIr_2Si_2$ the magnetic moment is parallel to the *c*-axis while in $TbIrSi_3$ it is perpendicular.

According to the prediction of Greedan and Rao [17,18], if the magnetic moment is parallel to the *c*-axis, the B_2^0 (the crystalline electric field parameter) is negative, and when it is perpendicular to the *c*-axis the B_2^0 is positive. For *I*-$TbIr_2Si_2$, the *B* is negative (−3.91 K) [19] while for the isostructural $DyIrSi_3$ compound the *B* parameter is positive [9]. The determined orientation of the magnetic moments in $TbIrSi_3$ suggests that for this compound the B_2^0 parameter is positive. The reduced value of the Tb magnetic moment in respect to the free Tb^{3+} ion value (equal 9 μ_B) is attributed to crystal-electric-field effects.

A change of the magnetic structure with the temperature observed in the $TbIrSi_3$ compound was detected in many

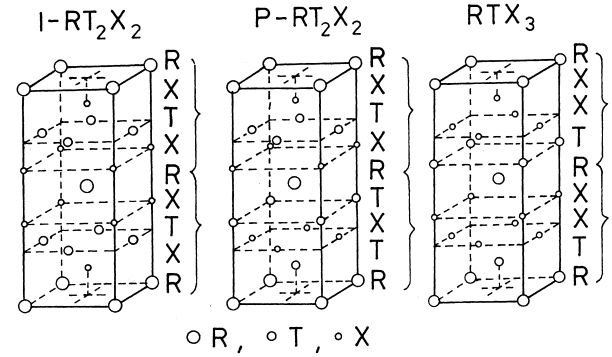

Fig. 6. The tetragonal cells of (a) the $ThCr_2Si_2$-type (space group *I4*/*mmm*), (b) the $CaBe_2Ge_2$-type (space group *P4*/*nmm*), and (c) $BaNiSn_3$-type (space group *I4mm*).

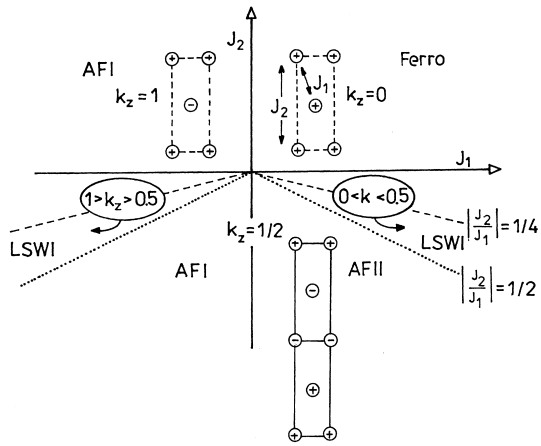

Fig. 7. Stability conditions of the $R(T,X)_4$ ternary compounds for the exchange integrals J_1 and J_2 [21,22].

intermetallic compounds [20]. The change of the magnetic structure from an incommensurate to a long-period commensurate can be interpreted using a realistic mean field which includes periodic-exchange-field and crystal-field effects.

The observed change of the $TbIrSi_3$ magnetic structure can be explained on the basis of the following simple model. In both observed magnetic phases the interactions in the (001) planes are ferromagnetic, whereas the exchange coupling J_1 and J_2, between the first and the second planes perpendicular to the *c*-axis are weak and antiferromagnetic. The predicted magnetic arrangements are shown in Fig. 7.

For a negative value of J_1 exchange and positive or negative value of J_2 exchange as well as for $J_2<J_1/4$, an antiferro-AFI magnetic structure is stable.

For $J_1/4<J_2<J_1/2$, the modulated magnetic ordering with a wave-vector $k=(0,0,k_z)$, is stable. The values of the k_z component are given by the relation $\cos \pi k_z=-J_1/4J_2$. For $TbIrSi_3$, the k_z is: $0.5<k_z<1.0$ which indicates that both J_1 and J_2 integrals are negative. The magnetic phase diagram is shown in Fig. 2 [21,22].

The obtained results suggest that with an increasing temperature, a change of the exchange integrals is observed.

Acknowledgements

This work has been partially supported by the European Commission through the PECO 93 Action (contract: ERB CIPD CT 940088) and for the State Committee for Scientific Research in Poland in the frame of the Grant 2 P03 B087 08.

References

[1] K.R. Andress, E. Alberti, Z. Metallkd. 27 (1935) 12.
[2] Z. Ban, M. Sikirica, Acta Crystallogr. 18 (1965) 594.
[3] B. Eisenmann, N. May, W. Müller, H. Schafer, Z. Naturforsch. B27 (1973) 1155.
[4] W. Dorrscheidt, H. Schafer, J. Less-Common. Met. 58 (1978) 209.
[5] A. Szytuła, J. Leciejewicz, in: K.A. Gschneidner Jr., L. Eyring (Eds.), Handbook on the Physics and Chemistry of Rare Earths, vol. 12, North Holland, Amsterdam, 1989, p. 133.
[6] A. Szytuła, in: K.H.J. Buschow (Eds.), Handbook of Magnetic Materials, vol. 6, Elsevier, Amsterdam, 1991, p. 83.
[7] A. Szytuła, J. Leciejewicz, Handbook of Crystal Structures and Magnetic Properties of Rare Earth Intermetallics, CRC Press, Boca Raton, 1994.
[8] P. Hean, P. Lejay, B. Chevalier, B. Lloret, J. Etourneau, M. Sera, J. Less-Commom Met. 110 (1985) 321.
[9] J.P. Sanchez, K. Tomala, K. Łątka, J. Magn. Magn. Mater. 99 (1991) 95.
[10] T. Jaworska-Gołąb, M. Guillot, M. Kolenda, E. Ressouche, A. Szytuła, J. Magn. Magn. Mater. 164 (1996) 371.
[11] Wang Xian-Zhong, B. Lloret, Ng. Wee Lam, B. Chevalier, J. Etourneau, P. Hogenmuller, Revue de Chimie Minérale 22 (1985) 711.
[12] J. Rodriguez-Carvajal, Physica B 192 (1993) 55.
[13] V.F. Sears, Neutron News 3 (1992) 26.
[14] A.J. Freeman, J.P. Desclaux, J. Magn. Magn. Mater. 12 (1979) 11.
[15] M. Hirjak, B. Chevalier, J. Etourneau, P. Hagenmuller, Mat. Res. Bull. 19 (1984) 727.
[16] M. Ślaski, A. Szytuła, J. Leciejewicz, J. Magn. Magn. Mater. 39 (1983) 268.
[17] J.E. Greedan, V.U.S. Rao, J. Solid-state Chem. 6 (1973) 387.
[18] J.E. Greedan, V.U.S. Rao, J. Solid-state Chem. 8 (1973) 386.
[19] K. Łątka, Rep. INP 1443/PS, Kraków, 1989.
[20] D. Gignoux, D. Schmitt, Phys. Rev. B 48 (1993) 12692.
[21] A. Szytuła, W. Bażela, J. Leciejewicz, Solid-state Commun. 48 (1983) 1053.
[22] R. Welter, Thesis, University of Nancy, 1994.